

# THE RECEPTOR–TOXIN–ANTIBODY INTERACTION: MATHEMATICAL MODEL AND NUMERICAL SIMULATION

P. Katauskis<sup>1</sup>, P. Skakauskas<sup>1</sup>, A. Skvortsov<sup>2</sup>

<sup>1</sup>*Vilnius University, Lithuania*

<sup>2</sup>*DSTO, VIC 3207, Melbourne, Australia*

E-mail: pranas.katauskis@mif.vu.lt, vladas.skakauskas@maf.vu.lt,  
alex.skvortsov@dsto.defence.gov.au

## 1 Introduction

An antibody, also known as an immunoglobulin, is a protein used by the immune system to identify, neutralize, or kill foreign 'intruders' like bacteria, viruses, or pollen which are termed as antigen. The production of antibodies is the main function of the immune system. An antigen, when introduced into the body, triggers the production of an antibody by immune system which will then kill or neutralize the antigen that is recognized as a foreign invader.

The bio-medical application of antibodies against an effect of toxins associated with various biological threats (epidemic outbreaks or bio-terrorism) is well-documented (see, e.g., [1–3]).

For a long time the main target of antibody design has been the antibody affinity. With progress in bio-engineering, many antibodies with different affinity parameters have been generated. However, according Skvortsov and Gray [4] affinity is not a good predictor of protective or therapeutic potential of an antibody. In fact, the treatment effect of an antibody can be described by a parameter which includes the reaction rates of the receptor-toxin-antibody (RTA) kinetics and relative concentration of reacting species. As a result, any given value of this parameter determines a range of antibody kinetic properties and its relative concentration in order to achieve a desirable therapeutic effect.

The model considered by Skvortsov and Gray is a model of well-mixed solution of toxin, antibody, and cells and neglects diffusion fluxes of interacting species. Diffusion fluxes are significant especially when process of RTA interaction is limited by diffusion. Skakauskas et al. [5] examined numerically a RTA interaction model taking into account diffusion of all species in the case where a spherical cell is embedded into an initially uniformly distributed toxin–antibody solution which occupies a large volume (compartment) lying between the cell and external surface. Initial values of species and their values on the external surface were assumed to be the same for all times. In this case fluxes of toxin, antibody and their complex across the external surface are not zero. Some numerical results of the evaluation of an antibody treatment efficiency parameter are given in this paper.

In the present paper by using the same model we study an influence of the RTA kinetic parameters and diffusivity of toxin, antibody, and their complex on the behavior of the antibody protection parameter and concentrations of species in more detail.

The paper is organized as follows. In Section 2 we introduce the reaction–diffusion model for RTA interaction. Numerical results are presented in Section 3. Summarizing remarks given in Section 4 conclude the paper.

## 2 The model

We study a case of a spherical cell embedded into a toxin–antibody solution which occupies an extracellular domain  $\Omega$  lying between the cell and an external surface and use notations of paper [5]:

$\rho$  – spherical radius,

$S_c = \{\rho : \rho = \rho_c\}$  – the surface of the spherical cell,  $\rho_c$  is its radius,

$S_e = \{\rho : \rho = \rho_e\}$  – the surface of the external sphere (external surface of  $\Omega$ ),  $\rho_e$  is its radius,

$\Omega = \{\rho : \rho \in (\rho_c, \rho_e)\}$  – the extracellular domain,

$r_0$  – the concentration of receptors on the cell surface,

$\theta(t, \rho)$  – the fraction of the toxin-bound receptors,

$r_0\theta$  – the concentration of the toxin-bound receptors (confined to  $S_c$ ),

$r_0(1 - \theta)$  – the concentration of the free receptors,

$u_T$ ,  $u_A$ , and  $u_C$  – the concentrations of toxin, antibody, and toxin–antibody complex, respectively,

$u_T^0$ ,  $u_A^0$ ,  $u_C^0$  – the initial concentrations,

$\kappa_T, \kappa_A$ , and  $\kappa_C$  – the diffusivity of the toxin, antibody, and toxin–antibody complex, respectively,

$k_1, k_{-1}$  – the forward and reverse constants of the toxin–antibody reaction rate,

$k_2$  and  $k_{-2}$  – the forward and reverse constants of the toxin and receptor binding rate,

$k_3$  – the rate constant of the toxin internalization,

$\partial_n$  – the outward normal derivative on  $S_e$  or  $S_c$ ,

$\partial_t = \partial/\partial t$ ,

$\Delta = \rho^{-2} \frac{\partial}{\partial \rho} (\rho^2 \frac{\partial}{\partial \rho})$  – the Laplace operator,

$\psi(t)$  – the antibody protection factor (a relative reduction of toxin inside a cell due to application of antibody).

Dynamics of the concentrations  $u_T, u_A, u_C$ , and  $\theta$  can be described by the following equations:

$$\begin{cases} \partial_t u_T = -k_1 u_T u_A + k_{-1} u_C + \kappa_T \Delta u_T, & \rho \in \Omega, t > 0, \\ u_T = u_T^0, & \rho = \rho_e, t > 0, \\ \partial_n u_T = \frac{r_0}{\kappa_T} (-k_2(1-\theta)u_T + k_{-2}\theta), & \rho = \rho_c, t > 0, \\ u_T|_{t=0} = u_T^0, & \rho \in \Omega, \end{cases} \quad (1)$$

$$\begin{cases} \partial_t \theta = k_2(1-\theta)u_T - k_{-2}\theta - k_3\theta, & \rho = \rho_c, t > 0, \\ \theta|_{t=0} = 0, & \rho = \rho_c, \end{cases} \quad (2)$$

$$\begin{cases} \partial_t u_A = -k_1 u_T u_A + k_{-1} u_C + \kappa_A \Delta u_A, & \rho \in \Omega, t > 0, \\ u_A = u_A^0, & \rho = \rho_e, t > 0, \\ \partial_n u_A = 0, & \rho = \rho_c, t > 0, \\ u_A|_{t=0} = u_A^0, & \rho \in \Omega, \end{cases} \quad (3)$$

$$\begin{cases} \partial_t u_C = k_1 u_T u_A - k_{-1} u_C + \kappa_C \Delta u_C, & \rho \in \Omega, t > 0, \\ u_C = 0, & \rho = \rho_e, t > 0, \\ \partial_n u_C = 0, & \rho = \rho_c, t > 0, \\ u_C|_{t=0} = 0, & \rho \in \Omega. \end{cases} \quad (4)$$

The initial and boundary conditions to the system above correspond to a case where initially the toxin and antibody are distributed uniformly in the extracellular domain  $\Omega$ . Values of all species on the outer boundary of  $\Omega$  for all times and their initial values are assumed to be the same. In particular, zero value of the toxin–antibody complex is used for initial time and for all times on the outer boundary of  $\Omega$ . We stress that in this case the fluxes of all species are not zero on the outer boundary  $S_e$  of  $\Omega$ .

Eqs. (1)–(4) can be presented in non-dimensional form by using scales of  $\tau_*$  (time),  $l$  (length), and  $u_*$  (concentration). By substituting variables  $x = l\bar{x}$ ,  $t = \tau_*\bar{t}$ ,  $r_0 = lu_*\bar{r}_0$ ,  $u_T = u_*\bar{u}_T$ ,  $u_A = u_*\bar{u}_A$ ,  $u_C = u_*\bar{u}_C$ ,

$u_{T0} = u_*\bar{u}_T^0$ ,  $u_{A0} = u_*\bar{u}_A^0$ ,  $\bar{k}_1 = \tau_*u_*k_1$ ,  $\bar{k}_2 = \tau_*u_*k_2$ ,  $\bar{k}_{-1} = \tau_*k_{-1}$ ,  $\bar{k}_{-2} = \tau_*k_{-2}$ ,  $\bar{k}_3 = \tau_*k_3$ ,  $\bar{\kappa}_T = \tau_*\kappa_T l^{-2}$ ,  $\bar{\kappa}_A = \tau_*\kappa_A l^{-2}$ ,  $\bar{\kappa}_C = \tau_*\kappa_C l^{-2}$  into (1)–(4) we can deduce the same system, but only in the non-dimensional variables. Therefore, for simplicity in what follows, we treat system (1)–(4) as non-dimensional.

The main antibody treatment efficiency parameter is the antibody protection factor (a relative reduction of toxin attached to a cell due to application of antibody) which can be defined by the following expression [4,5]:

$$\psi(t) = \frac{\int_{S_c} \theta|_{u_A^0 > 0} dS}{\int_{S_c} \theta|_{u_A^0 = 0} dS}. \quad (5)$$

By definition  $0 \leq \psi \leq 1$ . The lower values of  $\psi$  the more profound therapeutic effect of antibody treatment.

### 3 Numerical results

We treated system (1)–(4) numerically for the spherically symmetric domain,  $\rho \in (\rho_c, \rho_e)$ , and  $t > 0$  with an implicit finite-difference scheme. Our selection of the values of parameters was motivated by the values available in the literature [3,5–7] with the extended RTE to allow exploration and illustration of the various transport and kinetics regimes that are possible in the RTA system. We employ the following data that were used in the most calculations in [5,8]:  $u_* = 6.02 \cdot 10^{13} \text{ cm}^{-3}$ ,  $\tau_* = 1 \text{ s}$ ,  $r_0 = 1.6 \cdot 10^4 / S_c$ , where  $1.6 \cdot 10^4$  is the total number of receptors of the cell,  $l = 10^{-2} \text{ cm}$ ,  $S_c = 4\pi\rho_c^2 = 4\pi \cdot 10^{-6} \text{ cm}^2$ ,  $\bar{r}_0 = 2.115 \cdot 10^{-3}$ . The standard non-dimensional values of the other parameters are the following:

$$\begin{cases} k_1 = 1.3 \cdot 10^{-2}, & k_{-1} = 1.4 \cdot 10^{-4}, \\ k_2 = 1.25 \cdot 10^{-2}, & k_{-2} = 5.2 \cdot 10^{-4}, & k_3 = 3.3 \cdot 10^{-5}, \\ \kappa_T = 10^{-2}, & \kappa_A = 10^{-2}, & \kappa_C = 10^{-2}, \\ \rho_c = 10^{-1}, & \rho_e = 2, \\ u_A^0 = 1, & u_T^0 = 0.5. \end{cases} \quad (6)$$

These values correspond to the ricin and 2B11 mono-clonal antibody interaction. If values of  $k_1$ ,  $k_2$ ,  $\kappa_A$ ,  $\kappa_C$ , and  $\kappa_T$  differ from those given in (6), they are specified in the legends of plots.

As we indicated in the Introduction, the main purpose of our study was to estimate the effect of diffusive and kinetic parameters of species on the behavior of concentrations of species and protective properties of an antibody against a toxin. Results of numerical solving of system (1)–(4) are presented in Figs. 1–7.

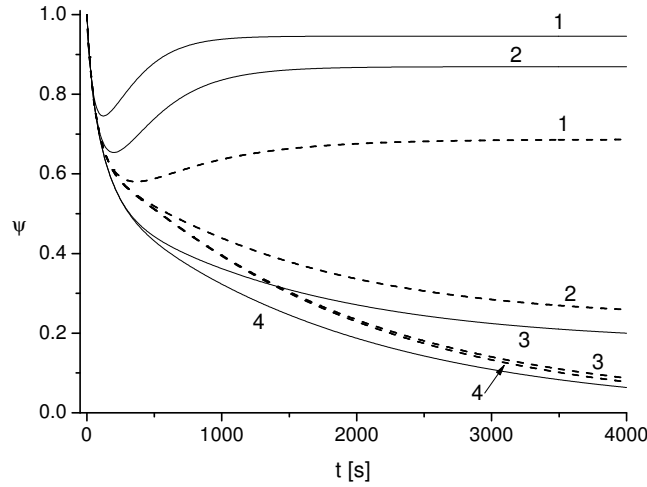


Fig. 1. Influence of the external radius  $\rho_e = 2$  (solid line) and 5 (dashed line) and the toxin diffusivity  $\kappa_T : 10^{-2}$  (1),  $5 \cdot 10^{-3}$  (2),  $10^{-3}$  (3),  $10^{-4}$  (4) on the cell protection characteristic,  $\psi$ , in the case of  $u_T^0 = 0.6$ .

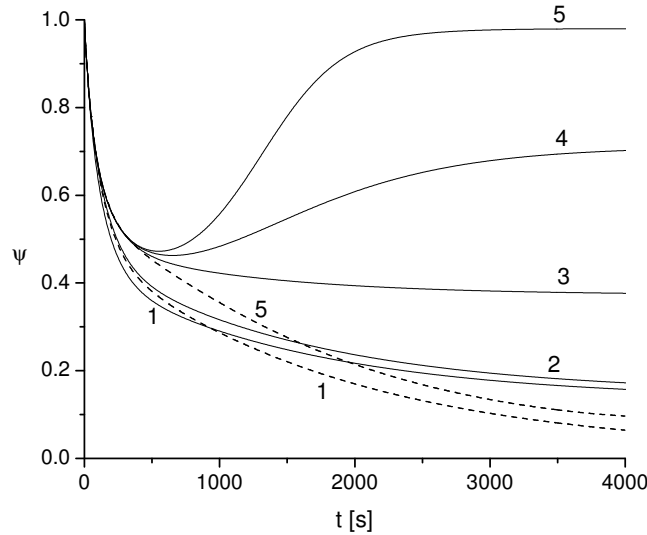


Fig. 2. Effect of the external radius  $\rho_e = 2$  (solid line) and 5 (dashed line) and the antibody diffusivity  $\kappa_A : 10^{-1}$  (1),  $10^{-2}$  (2),  $10^{-3}$  (3),  $5 \cdot 10^{-4}$  (4),  $10^{-4}$  (5) on the cell protection factor,  $\psi$ , in the case of  $\kappa_T = 10^{-3}$ .

The plots of  $\psi$  in Fig. 1 depict the dependence of the antibody protection factor on the radius  $\rho_e$  of the external surface  $S_e$  and toxin diffusivity  $\kappa_T$ . Parameter  $\psi$  increases with  $\kappa_T$  growing, but its behavior for large values of  $\kappa_T$  is non-monotonic. For large values of  $\kappa_T$ , parameter  $\psi$  grows as  $\rho_e$  decreases. But for small values of  $\kappa_T$  its behavior is different. For example, if  $\kappa_T = 10^{-3}$ , then values of  $\psi$  for  $\rho_e = 5$  are larger than those for  $\rho_e = 2$  if  $t < 1400$  s approximately. But if  $\kappa_T \leq 10^{-4}$ , then, for all  $t$ , values of  $\psi$  for  $\rho_e = 5$  are larger than those for  $\rho_e = 2$  (see curves 3 and 4).

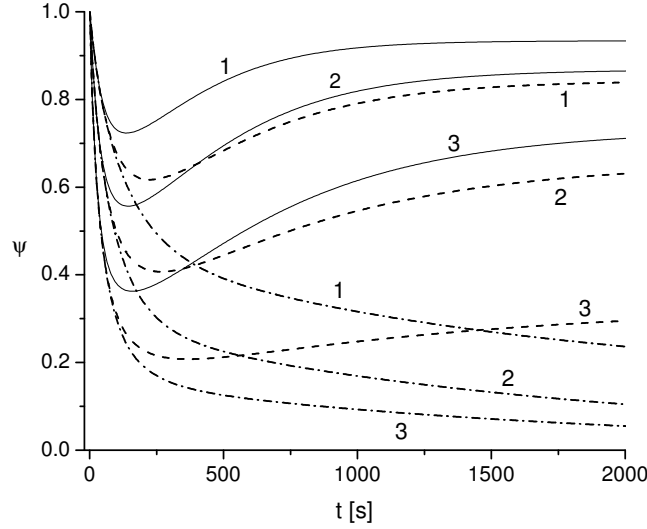


Fig. 3. Effect of the toxin diffusivity  $\kappa_T$  :  $10^{-2}$  (solid line),  $5 \cdot 10^{-3}$  (dashed line),  $10^{-3}$  (dash-dotted line) and parameter  $k_1$  :  $1.3 \cdot 10^{-2}$  (1),  $2 \times 1.3 \cdot 10^{-2}$  (2),  $4 \times 1.3 \cdot 10^{-2}$  (3) on the cell protection function  $\psi$ .

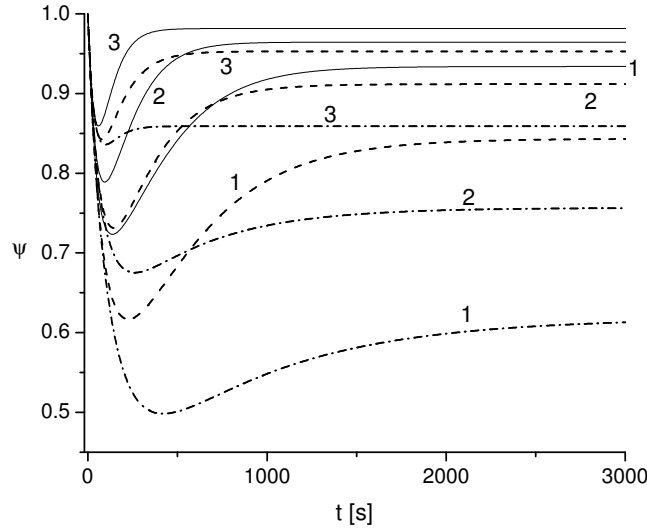


Fig. 4. Effect of the toxin diffusivity  $\kappa_T$  :  $10^{-2}$  (solid line),  $5 \cdot 10^{-3}$  (dashed line),  $2.5 \cdot 10^{-3}$  (dash-dotted line) and parameter  $k_2$  :  $1.25 \cdot 10^{-2}$  (1),  $2 \times 1.25 \cdot 10^{-2}$  (2),  $4 \times 1.25 \cdot 10^{-2}$  (3) on the cell protection function  $\psi$ .

Fig. 2 illustrates the dependence of  $\psi$  on the diffusivity  $\kappa_A$  of the antibody. The curves in this figure depict the increase of  $\psi$  as  $\kappa_A$  decreases and non-monotonic time evolution of  $\psi$  for small values of  $\kappa_A$ . Moreover, in the case of small antibody diffusivity,  $\kappa_A = 10^{-4}$ , values of  $\psi$  for  $\rho_e = 2$  are larger than those for  $\rho_e = 5$ . But in the case of large antibody diffusivity,  $\kappa_A = 10^{-1}$ , values of  $\psi$  for  $\rho_e = 2$  are smaller than those for  $\rho_e = 5$ , only if  $t \leq 1000$  s. For  $t > 1000$  s they behave *vica versa*.

Figs. 3 and 4 exhibit the dependence of  $\psi$  on diffusivity  $\kappa_T$ , forward constant  $k_1$  of the toxin and antibody reaction rate, and forward constant  $k_2$  of the toxin and receptor binding rate, respectively. Fig. 3 demonstrates the decrease of  $\psi$  as  $k_1$  increases. But different values of  $k_1$  do not change the monotonic behavior of all curves in time. From Fig. 4 we see the non-monotonic behavior of  $\psi$  as  $k_2$  increases. Moreover,  $\psi$  increases with  $k_2$  increasing. The bottom of the hollow in Fig. 3 is located lower than that in Fig. 4. One can see in Fig. 4 that the effect of toxin diffusivity variation on protection factor is sensitive to changes of parameter  $k_2$ . Let us compare the minimal values of protection factor. In the case of  $k_2 = 1.25 \cdot 10^{-2}$ , the minimum of  $\psi$  is about 0.72 at  $\kappa_T = 10^{-2}$ , 0.62 at  $\kappa_T = 5 \cdot 10^{-3}$  and 0.5 at  $\kappa_T = 2.5 \cdot 10^{-3}$ , while the corresponding values of  $\psi$  are about 0.86, 0.84 and 0.836 in the case of  $k_2 = 5 \cdot 10^{-2}$  (curves 1 and 3).

Numerical experiments show that diffusivity  $\kappa_C$  practically does not influence the time evaluation of  $\psi$ .

The plots of  $u_T$  in Fig. 5 depict the dependence of the toxin concentration at the cell surface on the diffusivity  $\kappa_T$  and radius  $\rho_e$  of the external surface  $S_e$ . For any value of  $\rho_e$ ,  $u_T$  decreases with  $\kappa_T$  decreasing. For large values of  $\kappa_T$ , function  $u_T(t, \rho_e)$  grows as  $\rho_e$  decreases. But, for small values of  $\kappa_T$ , its behavior is different. For example, for  $\kappa_T = 10^{-3}$ , values of  $u_T(t, \rho_e)$  for  $\rho_e = 5$  are larger than those for  $\rho_e = 2$  only if  $t < 500$  s (see

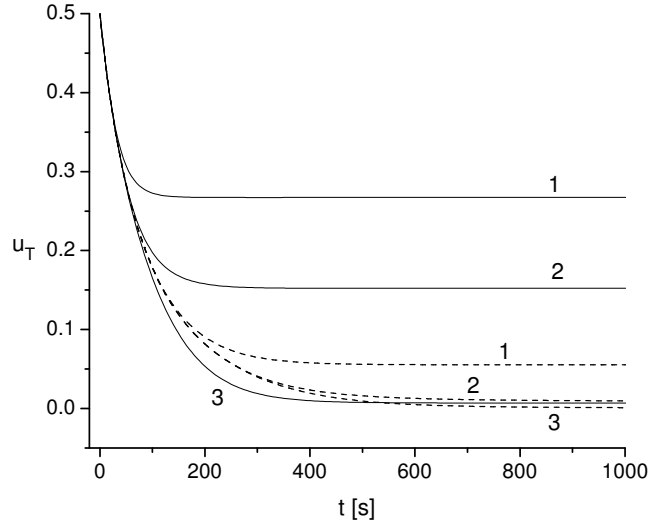


Fig. 5. Dynamics of toxin concentration  $u_T$  for  $\rho_e = 2$  (solid line),  $\rho_e = 5$  (dashed line), and  $\kappa_T : 10^{-2}$  (1),  $5 \cdot 10^{-3}$  (2),  $10^{-3}$  (3).

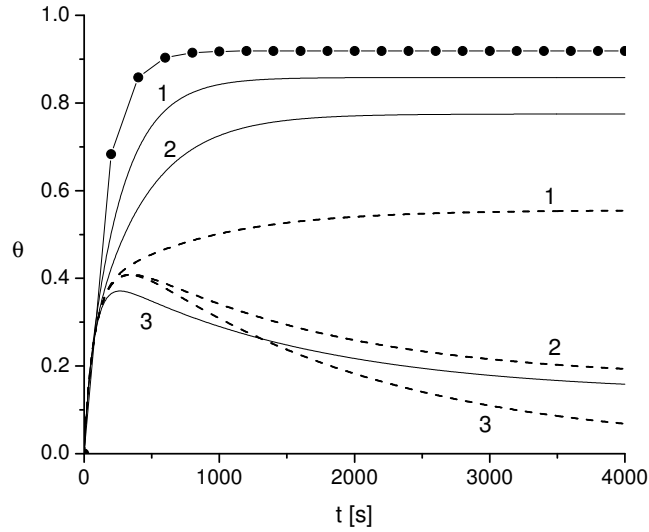


Fig. 6. Profiles of functions  $\theta$  for  $u_A^0 = 1$ ,  $\rho_e = 2$  (solid line);  $u_A^0 = 1$ ,  $\rho_e = 5$  (dashed line), and  $\kappa_T : 10^{-2}$  (1),  $5 \cdot 10^{-3}$  (2),  $10^{-3}$  (3). Line with bullets in the case of  $u_A^0 = 0$ .

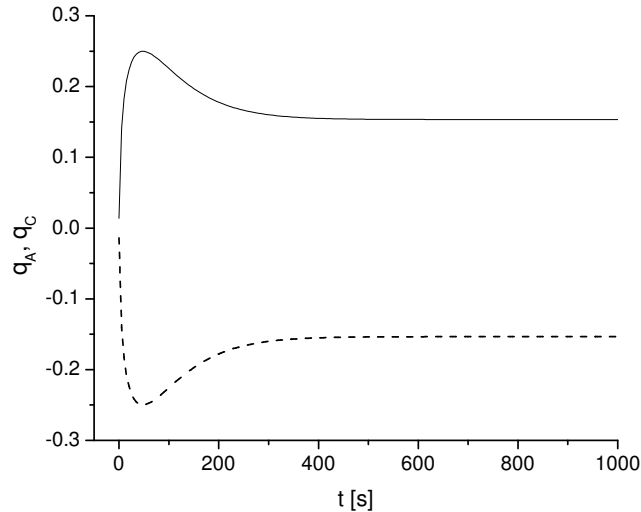


Fig. 7. Dynamics of functions  $q_A = \partial u_A(t, \rho_e) / \partial \rho$  and  $q_C = \partial u_C(t, \rho_e) / \partial \rho$  at  $\rho_e = 2$  for  $\kappa_T = 10^{-3}$  and  $\kappa_A = \kappa_C = 10^{-2}$ .

curves 3). Our calculations show that influence of  $\kappa_C$  on the behavior of  $u_T(t, \rho_c)$  is insignificant. We observed the non-monotonic behavior of  $u_T(t, \rho_c)$  for small  $\kappa_C$ , but difference between its steady-state value and value at the bottom of the hollow is very small (of order  $10^{-3}$ ).

Calculations show that  $u_C(t, \rho_c)$  grows with  $\kappa_C$  decreasing. The behavior  $u_C(t, \rho_c)$  is monotonic for  $\kappa_C \leq 5 \cdot 10^{-2}$ . Its values are smaller than initial ones of toxin for  $\kappa_C \in [5 \cdot 10^{-3}, 5 \cdot 10^{-2}]$ . But  $u_C(t, \rho_c)$  can reach a relatively large steady-state value for small  $\kappa_C$  while steady-state values of  $u_T$  and  $u_A$  are smaller than their initial values. For example, the steady-state value of  $u_C$  on  $S_e$  is equal to 2.2 for  $\kappa_C = 10^{-3}$ ,  $\kappa_A = \kappa_T = 10^{-2}$ . Derivatives of  $u_T$  and  $u_A$  with respect to  $\rho$  on  $S_e$  are of order 0.3 while derivative of  $u_C$  on  $S_e$  is of order  $-3$ . This means that  $u_C$  grows faster going towards the cell then grow  $u_T$  and  $u_A$  going out the extracellular domain.

Curves in Fig. 6 depict the dependence of  $\theta$  on  $\kappa_T$  and  $\rho_e$  for  $u_A^0 = 1$  and  $u_A^0 = 0$ . In the case where the antibody is absent values of  $\theta$  practically do not depend on diffusivity  $\kappa_T$  (see the bullets marked curve).  $\theta$  decreases with  $\kappa_T$  decreasing. For any  $\rho_e$ , function  $\theta$  grows as  $\kappa_T$  increases. If  $\kappa_T \in 5 \cdot [10^{-3}, 10^{-2}]$ , then values of  $\theta$  for  $\rho_e = 2$  are larger than those for  $\rho_e = 5$ . But for small values of  $\kappa_T$  its behavior is different. For example, if  $\kappa_T = 10^{-3}$ , values of  $\theta$  for  $\rho_e = 5$  are larger than those for  $\rho_e = 2$  only for about  $t < 1300$  s. This behavior is similar to those of  $u_T$  and  $\psi$ .

Two curves in Fig. 7 illustrate the non-monotonic behavior of derivatives  $\partial u_A(t, \rho_e)/\partial \rho$  and  $\partial u_C(t, \rho_e)/\partial \rho$  for small toxin diffusivity ( $\kappa_T = 10^{-3}$ ). For  $\kappa_T = 10^{-2}$  their behave is monotonic.

## 4 Concluding remarks

To conclude the paper we summarize results of study. The receptor–toxin–antibody interaction is studied numerically by using a model proposed in [5]. The model includes ‘bulk’ reaction of toxin and antibody, surface binding of toxin and cell receptors, and diffusion of all species. The main results of the numerical study are the following:

1. The non-monotone evolution of concentrations of some species (toxin and toxin-bound receptors) and the antibody protection factor for some cases (large toxin diffusivity, small antibody diffusivity, and large forward constant of the toxin–receptor binding rate).
2. The influence of small or large values of  $\kappa_T$ ,  $\kappa_A$ , and  $k_2$  on the behavior of  $u_T(t, \rho_c)$ ,  $\theta(t)$  and  $\psi(t)$  is profoundly different in the cases of small or large  $\rho_e$ .
3. The effect of  $\kappa_C$  on the evolution of  $u_T$ ,  $\theta$ , and  $\psi$  was found to be insignificant.

## References

1. *Oral H.B., Ozakin C., Akdis C.A.* Back to the future: antibody-based strategies for the treatment of infectious diseases // *Mol. Biotechnol.* **21**, 225–239 (2002).
2. *Lobo E.D., Hansen R.J., Balthasar J.P.* Antibody pharmacokinetics and pharmacodynamics // *J. Pharm. Sci.* **93**, 2645–2668 (2004).
3. *Prigent J., Panigai L., Lamourette P., Sauvaire D., Devilliers K. et al.* Neutralising antibodies against ricin toxin // *PloS ONE.* **6**. e20166 (2011)
4. *Skvortsov A., Gray P.* Modeling and simulation of receptor–toxin–antibody interaction // *Proc. 18th World IMACS/ MODSIM Congress.* Cairns, Australia, 185–191, (2009)
5. *Skakauskas V., Katauskis P., Skvortsov A.* A reaction–diffusion model of the receptor–toxin–antibody interaction // *Theor. Biol. Med. Model.*, **8/32**, 1–15 (2011).
6. *Sandvig K., Olsnes S., Pihl A.* Kinetics of binding of the toxic lectins abrin and ricin to surface receptors of human cells // *J. Biol. Chem.* **251**, 3077–3984 (1976)
7. *Lectures Notes in Immunology: Antigen–antibody interactions*, Univ. Pavia.  
[http : //nfs.unipv.it/nfs/minf/dispense/immunology/lectures/files/antigens\\_antibodies.html](http://nfs.unipv.it/nfs/minf/dispense/immunology/lectures/files/antigens_antibodies.html) (2011).
8. *Truskey G.A., Yuan F., Katz D.F.* *Transport Phenomena in Biological Systems*, second ed. Prentice Hall, 888 pp, (2009).